Journal of Power Sources 240 (2013) 267–272

Contents lists available at SciVerse ScienceDirect

Journal of Power Sources

journal homepage: www.elsevier.com/locate/jpowsour

Short communication

Polypyrrole-covered MnO_2 as electrode material for supercapacitor

A. Bahloul [a,b,*], B. Nessark [a], E. Briot [b], H. Groult [b], A. Mauger [c], K. Zaghib [d], C.M. Julien [b]

[a] Université Ferhat Abbas, Laboratoire d'Electrochimie et Matériaux, Sétif 19000, Algeria
[b] Université Pierre et Marie Curie, PECSA, UMR 7195, Bat. F, 4 place Jussieu, 75005 Paris, France
[c] Université Pierre et Marie Curie, IMPMC, 4 place Jussieu, 75005 Paris, France
[d] Energy Storage and Conversion, Research Institute of Hydro-Québec, Varennes, Québec, Canada J3X 1S1

HIGHLIGHTS

- γ-MnO_2 as hybrid electrode material in aqueous asymmetric super-capacitor.
- Blend formed by electrochemical polymerization of pyrrole monomer (PPy).
- Enhancement of the specific capacitance by a factor 2 for PPy/MnO_2 electrode.

ARTICLE INFO

Article history:
Received 11 February 2013
Received in revised form
3 April 2013
Accepted 4 April 2013
Available online 10 April 2013

Keywords:
Manganese dioxide
Electrodeposition
Super-capacitors
Polypyrrole

ABSTRACT

γ-MnO_2 has been synthesized by hydrothermal process, and studied as electrode material in aqueous asymmetric super-capacitor. We studied the blend formed by electrochemical polymerization of pyrrole deposited onto γ-MnO_2 particles. The composite materials (PPy/MnO_2) were characterized by different methods including cyclic voltammetry, chronoamperometry, X-ray diffractometry and BET measurements. The specific capacitance at constant current density 2 mA cm^{-2} was calculated from galvanostatic charge-discharge cycling tests. The asymmetric super-capacitor using (PPy/MnO_2) composite material has high specific capacitance of 141.6 F g^{-1} compared with 73.7 F g^{-1} for γ-MnO_2 before PPy coating. The improvement of the coating is not only due to the electronic conductivity of the polymer, but also due to an increase of the BET surface area that raises to 125 m^2 g^{-1} after coating, against 64 m^2 g^{-1} for pristine MnO_2.

© 2013 Elsevier B.V. All rights reserved.

1. Introduction

Electrochemical super-capacitors are novel devices for energy storage, which fill the gap in the power density between batteries and dielectric capacitors [1,2]. Their properties have been reviewed in different books [3,4]. Among them, pseudo-capacitors are devices based on electrode charge storage. Their performance depends on highly reversible Faradaic electrochemical redox surface processes and, when the electrodes are based on conducting polymers, on the thickness of the polymer. Amorphous $RuO_2 \bullet nH_2O$ is the best example of pseudo-capacitor electrode, with specific capacitance 863 F g^{-1} [5]. However, the high cost of such a metal oxide has stimulated researchers to identify cheaper materials that exhibit similar behavior. Among them, MnO_2 possesses the advantages of low cost, sufficiently high specific capacitance, and is environmentally friendly, which was the motivation for the numerous studies devoted to this material as electrode material in aqueous asymmetric super-capacitor [6–8], reviewed in Refs. [9–11].

The capacitance of the MnO_2 electrode is believed to be mainly due to reversible redox transitions involving exchange of protons and/or cations with the electrolyte [12,13]. However, the resistivity and the equivalent series resistance (ESR) of MnO_2 electrode are very large. In theory, if one Mn atom in MnO_2 is assumed to store one electron, then the specific capacitance of MnO_2 should be around 1370 F g^{-1} [14]. In practice, however, the experimental values of the specific capacitance for pure MnO_2 is limited to 135 F g^{-1} for thick films [7,15], reaching 166 F g^{-1} for amorphous MnO_2 [16]. This is mostly due to the intrinsically poor electronic conductivity of MnO_2 (10^{-5}–10^{-6} S cm^{-1}), which remains a major challenge and limits the rate capabilities for high power performance [17,18]. To improve the electrical conductivity, Mn has been mixed with Ni, which increases the specific capacitance to 210 F g^{-1} [16], and considerable research efforts have been placed on

* Corresponding author. Université Ferhat Abbas, Laboratoire d'Electrochimie et Matériaux, Sétif 19000, Algeria.
E-mail address: cyberbahloul@yahoo.fr (A. Bahloul).

0378-7753/$ – see front matter © 2013 Elsevier B.V. All rights reserved.
http://dx.doi.org/10.1016/j.jpowsour.2013.04.013

exploring composite structures where MnO_2 is combined with highly conductive materials such as metal nanostructures [19], carbon nanotubes [20–23], graphene [24,25] or conducting polymers [26,27]. Brousse et al. evaluated the capacitances of different MnO_2 polymorphs and thus investigated the relationship between structure and electrochemical properties, revealing that amorphous and 2D birnessite MnO_2 were more competitive as electrode materials for supercapacitors [28]. On another hand, hydrothermal technique is a cheap, environmentally friendly method to prepare materials in different nano-architectures such as nanorods, nanowires and nanoparticles [29,30], and has thus also been used to synthesize MnO_2. In particular, a mixture of nanostructured particles with a distinct plate-like morphology and nanorods has been obtained in the α-MnO_2 phase [4]. Rod-shaped MnO_2 have also been obtained by another technique as a multi-crystal with a mixture of α-and γ-MnO_2 phases [31].

In this work, MnO_2 has been synthesized by hydrothermal method in the γ-phase, and modified by electro-polymerization of pyrrole to test its ability as a possible active electrode material in an aqueous electrochemical super-capacitor (SC). The polypyrrole (PPy) coating aims at obtaining a better contact between the particles and a good electronic conductivity of the electrode. The PPy/MnO_2 materials are characterized by X-ray diffractometry and Brunauer–Emmett–Teller (BET) measurements. Their electrochemical properties are investigated using cyclic voltammetry, chrono-amperometry and charge–discharge tests. The specific capacitance was calculated from galvanostatic charge–discharge cycling experiments.

2. Experimental

The MnO_2 particles were synthesized by hydrothermal method. Analytical-grade chemicals $MnCl_2{\cdot}4H_2O$ and $KMnO_4$, (from Acros Organics) were used as received without any further purification. 1.98 g of $MnCl_2{\cdot}4H_2O$ was dissolved in 50 mL of distilled water and 2.89 g of $KMnO_4$ dissolved in 50 mL distilled water was added upon stirring for about 20 min and preheated to 80 °C. The obtained brown-color precipitate was washed out with distilled water several times and dried in a vacuum oven at around 110 °C for 10 h. The specific surface area was estimated by BET analysis using a Quantasorb (Quantachrom) apparatus. The structure of the samples was investigated using an X-ray diffractometer (model Philips X'Pert) using nickel-filtered Cu–Kα radiation. The diffractograms were taken at room temperature in the 2θ-range 10–80°.

The electrochemical tests were carried out using a PC-controlled potentiostat (VOLTALAB 50, Radiometer). All cyclic voltammograms were recorded at room temperature, using a single compartment of a three-electrode cell. We have reported the preparation of the working electrode in a previous work [32]. MnO_2 powders were pressed on a bar carbon, 3 mm diameter inserted inside a Teflon tube, after the carbon was polished and rinsed with distilled water. The working electrode potentials were measured against an aqueous saturated calomel electrode (SCE). A pure carbon bar was used as counter electrode. The charge–discharge tests were carried out in a two-electrode cell using 1 M Na_2SO_4 as the electrolyte. The electrodes (20 mg) were prepared by mixing 70 wt.% MnO_2 powder as active material, 20 wt.% acetylene black (Alfa, >99.9%) and 10 wt.% graphite (Prolabo). The mixture was pressed on graphite current collector with a surface 1 cm^2. A glass paper separator was placed between the working electrode and the auxiliary electrode.

3. Results

Fig. 1 shows the typical X-ray diffraction (XRD) pattern of the as-prepared MnO_2. The XRD diagram is characterized by broad peaks

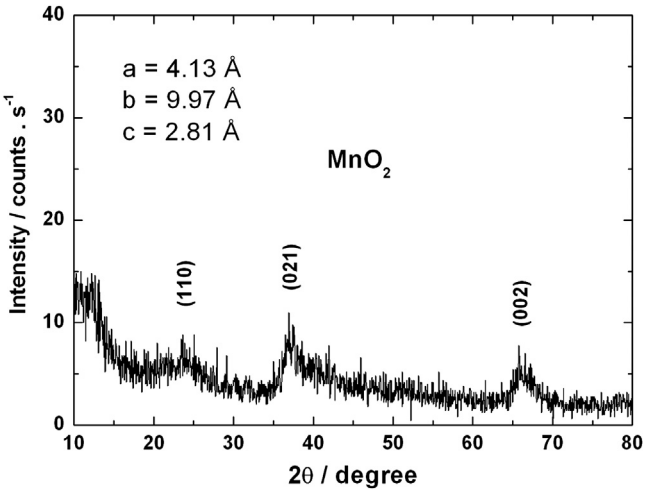

Fig. 1. XRD diffraction pattern of as-prepared MnO_2.

located at ca. 23.8, 37.29, 41.87 and 66.25°, which can be indexed according to the crystallographic variety γ-MnO_2. The crystal structure of γ-MnO_2 consists in a combination of octahedral MnO_6 units. Double chains of edge-sharing MnO_6 octahedra share corners [33], and form (1 × 1) and (1 × 2) tunnels that extend along the short crystallographic axis of the orthorhombic unit cell. The crystallographic parameters of the pristine MnO_2 sample calculated by least-square fit using the orthorhombic symmetry *Pbnm* space group of γ-MnO_2 are $a = 4.13$ Å, $b = 9.97$ Å, $c = 2.81$ Å, so that the volume of the unit cell is $V = 116.12$ Å^3. Moreover, the XRD spectrum remains unchanged after the electrodeposition. Therefore, the electrodeposition of PPy occurring as a very thin layer undetectable by XRD does not affect the core of the particles.

The SEM image of the MnO_2 particles before and after covering with PPy in Fig. 2 shows that the MnO_2 powder is made of porous MnO_2 particles of regular shape, with an average grain size 250 nm. Note that the electrochemical polymerization process does not change the morphology of the MnO_2 grains, but the coat of the particles with PPy smears out the roughness of the surface of the particles.

The electro-deposition of PPy was carried out following the procedure described in prior works [32,34], with chronoamperometry test at monomer oxidation potential 0.9 V *vs.* SCE. The chrono-amperogram displayed in Fig. 3 shows the variation of the current density with time. The formation of polypyrrole at this low voltage (0.9 V) takes a long time, but this cannot be avoided because the electrolyte could be oxidized at higher voltage, in which case the polymer film would be fissured [35]. This potential was chosen from the voltamperometry curve. The fast decrease of the current density observed from 0.16 mA cm^{-2} to a steady value lower than 0.01 mA cm^{-2} is representative of the starting oxidation of the monomer. After 40 min of electro-polymerization, the specific area of the particles of the PPy/MnO_2 final product was analyzed by BET and compared with the as prepared MnO_2 material. As a result, the BET surface area is 125 $m^2\ g^{-1}$, which is larger by 51% than that of pristine MnO_2 (64 $m^2\ g^{-1}$). This result gives evidence that the PPy deposit has covered the surface of the particles, a result that is consistent with the SEM images in Fig. 2.

The MnO_2 and the PPy/MnO_2 electrodes obtained after 1, 10, 20, and 40 min of electro-polymerization were subjected to galvanostatic charge–discharge cycling between 0 and 1 V *vs.* SCE in aqueous 1 mol L^{-1} Na_2SO_4 electrolyte, using carbon anode. Note the potential has been chosen small enough to make sure that the PPy coat does not oxidize, since this oxidation takes place at 1.2 V. The time dependence of the potential $E(t)$ during the first few cycles

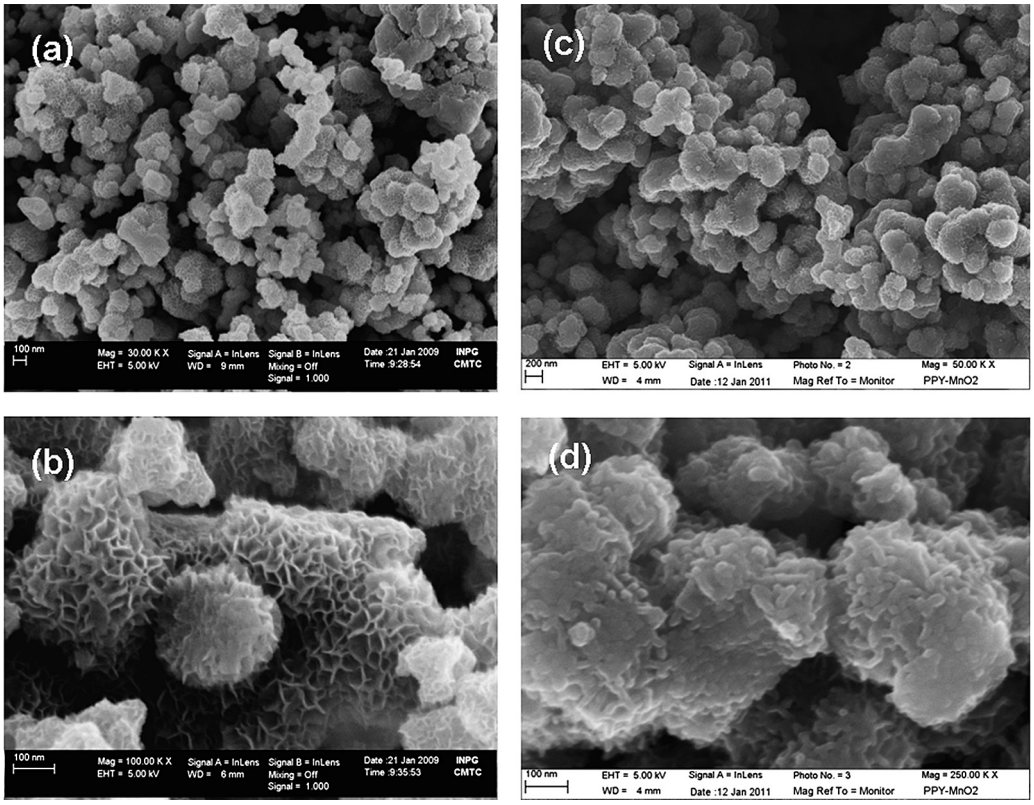

Fig. 2. SEM images of MnO_2 particles (left) and grains covered with PPy electrodeposited during 40 min (right), at two magnifications.

performed at current density $j = 2$ mA cm^{-2} is shown in Fig. 4. A pure capacitance behavior would lead to a linear variation of potential with time (with slope j/C with C the capacitance). This behavior, however, requires the rapid response of the interface to changes in electrode potential, which is characteristic of the electrochemical double layer capacitors (EDLC). This is not the case here, because of some saturation effect at the end of charge and discharge, giving evidence that the carbon used in this experiment does not play the role of the EDLC. We shall return to this problem in the discussion. At this point it is sufficient to note that the capacitance C can be deduced from the linear part of the $E(t)$ curve. The durations of charge and discharge are almost equal, meaning good reversibility. We can see in Fig. 4 that the charge–discharge time of the as-prepared MnO_2 is lower than that of PPy/MnO_2 materials prepared after the electro-deposition times of 1, 10, 20 and 40 min, reflecting the PPy coating effect. The PPy/MnO_2 sample prepared after 40 min has the maximum specific capacitance (SC) 141.6 F g^{-1}, while that of MnO_2 is 73.7 F g^{-1} only. The energy density of PPy/MnO_2 is then 12.6 Wh kg^{-1} and the power density available is 34 W kg^{-1}.

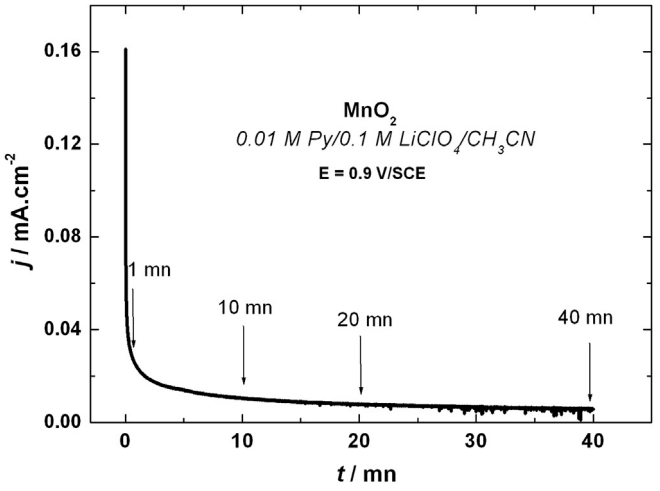

Fig. 3. The chronoamperometric response of prepared MnO_2 electrode in 0.01 mol L^{-1} Py/0.1 mol L^{-1} $LiClO_4$, submitted at potential 0.9 V *vs.* SCE.

Fig. 5 shows the galvanostatic charge–discharge curves obtained during the first cycle with the electrodes made of MnO_2 and PPy/MnO_2 prepared after 40 min, and measured in 1 mol L^{-1} Na_2SO_4 electrolyte at various current densities from 2 to 10 mA cm^{-2} by step of 2 mA cm^{-2}. The SC measured in the same way with MnO_2 and PPy/MnO_2 obtained after 20 and after 40 min of electro-deposition of PPy are reported in Table 1. The larger SC for PPy/MnO_2 is due to the improvement of the electronic conductivity between the particles, owing to their PPy coat. The SC decreases when the current density increases, which reflects the loss of efficiency of the active material at high current densities. The SC of MnO_2 and PPy/MnO_2 are reported in Table 1, for PPy/MnO_2 obtained after 20 and after 40 min of electro-deposition of PPy on MnO_2 particles. These results clearly show the positive effect of PPy electro-deposition on prepared MnO_2, which could be applied to other materials as electrode of pseudo-capacitors.

The MnO_2 and PPy/MnO_2 pseudo capacitance is due to the Mn^{4+}/Mn^{3+} reversible redox reaction; this process is accompanied by reversible insertion/extraction of alkali cation Na+ or protons H_3O^+ present in the electrolyte [6]:

$$MnO_2 + Na^+ + e^- \rightarrow MnOONa. \quad (1)$$

Note that the specific capacitance of PPy/MnO_2 materials is proportional to the thickness of the PPy deposit. To evaluate

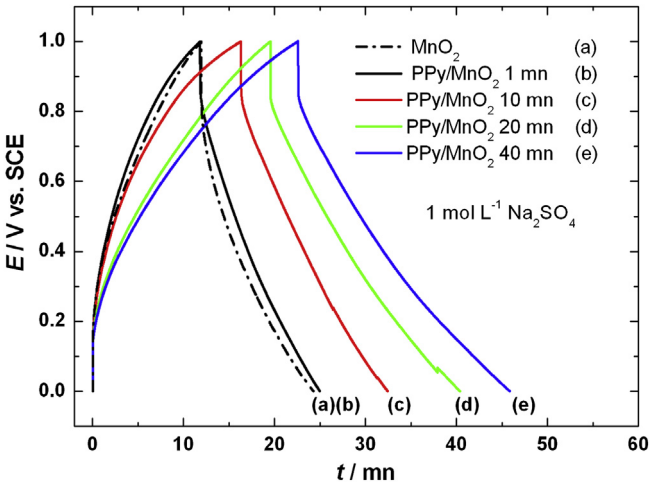

Fig. 4. Galvanostatic charge-discharge cycling at 2 mA cm^{-2} between 0 and 1 V *vs.* SCE in aqueous 1 mol L^{-1} Na_2SO_4 electrolyte of prepared MnO_2 (a) and PPy/MnO_2 (b) after 1, 10, 20 and 40 min of electropolymerization.

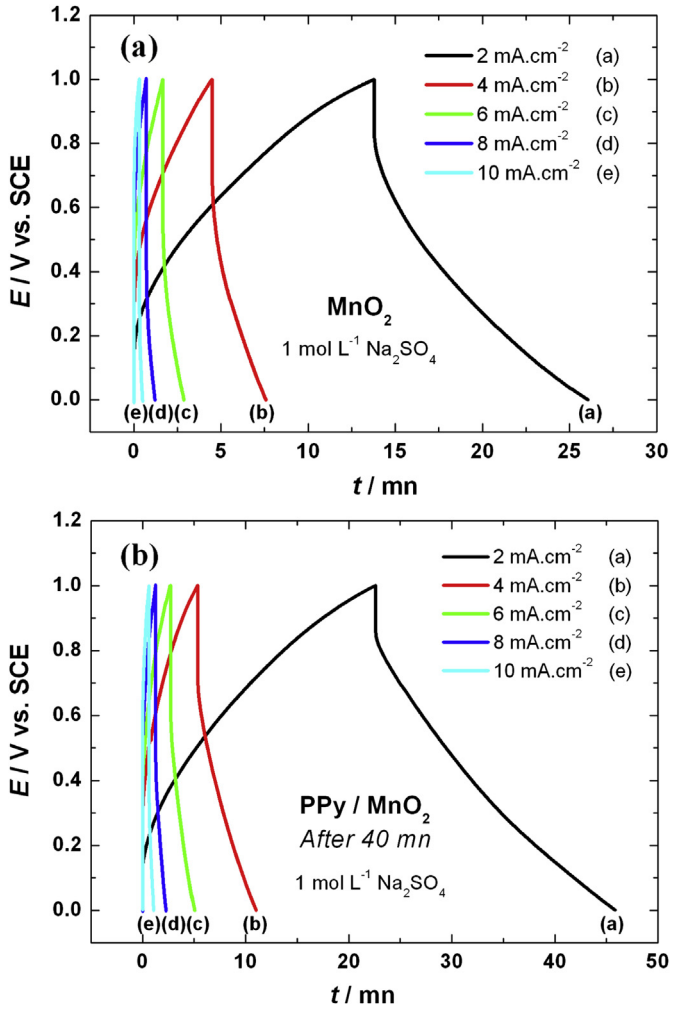

Fig. 5. Galvanostatic charge-discharge curves of MnO_2 (a) and PPy/MnO_2 (b) prepared after 40 min composites electrodes measured in 1 mol L^{-1} Na_2SO_4 electrolyte at various current densities of 2, 4, 6, 8 and 10 mA cm^{-2}.

the performance of the composite material, the specific capacitance of the C//PPy-MnO_2 capacitor was measured in a constant charging–discharging experiment at a discharge current density 2 mA cm^{-2} over 500 cycles on a sample obtained after 40 min of electro-deposition of PPy on MnO_2 (Fig. 6). The stabilization of specific capacitance indicates that the electrode has regular capacitive behavior and good cycling stability.

The beneficial effect of the electro-deposition of PPy can also be evidenced by the ac impedance measurements that have been carried out at open-circuit voltage using perturbation voltage amplitude 10 mV in the frequency range from 100 kHz to 50 mHz. The results reported in Fig. 7 for the MnO_2 sample before and after electro-deposition during 40 min have been analyzed following the procedure described in Ref. [36]. As a result, the charge transfer resistance that reaches 210 Ω cm^2 for the pristine sample decreases to 235 Ω cm^2 after the electro-deposition.

4. Discussion

Because of the very low conductivity of MnO_2, the content of the conducting material such as carbon included in the electrode is critical in obtaining a material with high electrochemical performance. Presence of carbon in the active material up to 20 wt.% creates an electric path between the oxide particles, thus increasing the number of active sites for the electrochemical faradaic reaction [37], and this amount of carbon is required to obtain *C–V* curves rectangular in shape, indicating a typical capacitor behavior [16]. Clearly, the low specific capacitance obtained before PPy-coating (73.7 F g^{-1}) shows that the 20 wt.% acetylene black (Alfa) fails to play this role. Actually, the specific capacitance of carbon ranges from 70 F g^{-1} for pure Black pearls 2000 [16] to 26 F g^{-1} for a commercial activated carbon for supercapacitors [31]. Therefore, the value of 73.7 F g^{-1} may even be overestimated, thus confirming that only few particles at the surface of the powder participate to the electrochemical process. This is in agreement with prior works showing a drop in capacitance and columbic efficiency on increasing film thickness [3,38]. Indeed, MnO_2 has improved specific capacitance only when deposited onto carbon nanotubes and conductive polymer like PPy [21,39,40], or ternary compounds involving both nanotubes and conductive polymers [41] in order to overcome the problem of inherent low conductivity. The simple coating of the γ-MnO_2 in the present work increases the specific capacitance up to 141.6 F g^{-1}, which is competitive with the results reported in the literature for the conventional slurry-pasted thick electrodes (>1 mg cm^{-2}) of pure MnO_2 particles without inclusion of very conductive additives. Actually, the specific capacitance compares well with that of amorphous MnO_2 considered as more performing than well crystallized MnO_2. The reason is that the deposit of PPy maintains crystallinity, which is critical to reduce grain boundaries and their resulting mass transfer effects [42].

Our results in the present work for γ-MnO_2 (141.6 F g^{-1} for a BET surface area 125 m^2 g^{-1}) are about the same as obtained for α-MnO_2 (168 F g^{-1} for a BET surface area 132 m^2 g^{-1} [4]). Therefore, we can conclude that the electrochemical performance of MnO_2 is essentially the same for the γ- and the α-MnO_2 varieties. It should

Table 1
Specific capacitance (SC) of MnO_2 and PPy/MnO_2 at different currents.

i (mA cm^{-2})	SC of MnO_2 (F g^{-1})	SC of PPy/MnO_2 after 20 min (F g^{-1})	SC of PPy/MnO_2 after 40 min (F g^{-1})
2	73.68	123.96	141.6
4	37.08	68.2	68.04
6	21.96	42.48	41.94
8	12.24	19.2	24.48
10	5.7	10.5	13.5

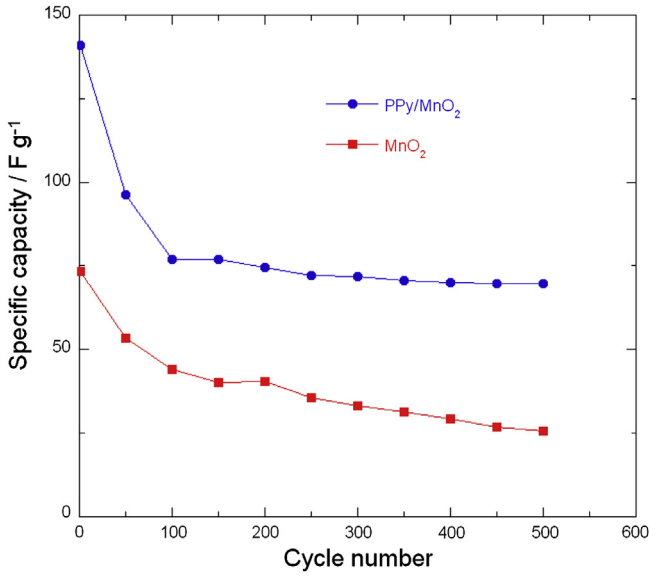

Fig. 6. The variation of specific capacitance of PPy/MnO_2 electrode *vs.* cycle number. Charge and discharge experiments were carried out at 2 mA cm^{-2}.

be noticed, however, that the morphology of the particles is different in these two cases. In the present work, the γ-MnO_2 particles are almost spherical, about 500 nm in diameter. On another hand, the SEM images of the α-MnO_2 particles in Ref. [4] show the presence of nanorods in addition to the 500 nm-thick particles. Therefore, the nanorods do not seem to play an important role in the samples of ref. [4]. This surprising result suggests that the weight of the nanorods is small with respect to that of the 500 nm thick particles. This result also gives evidence that the definite pores, which are comparable in the two cases as they lead to almost the same specific surface area, play the critical role in the redox process when MnO_2 is used as an electrode material in a supercapacitor. In addition, it is well known that only a thin layer (up to a few hundreds of nanometers) of oxide nanomaterials

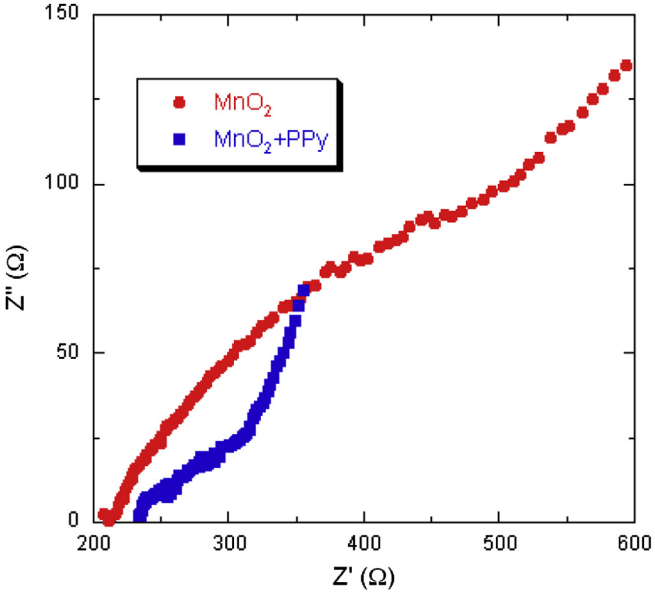

Fig. 7. Nyquist diagrams of pristine MnO2, and PPy/MnO2 after 40 min of electrodeposition of PPy.

participate efficiently in the charge storage process [17]. The results in the present work or in ref. [4] show that the size of the particles (500 nm) is still too thick. Indeed, high specific capacitance >600 F g^{-1} for MnO_2 are obtained only with MnO_2 ultra-thin films tens of nanometer thick [3,43,44], and 3-dimensional electrode designs in which nanoscopic MnO_2 deposits are incorporated directly onto the surface of nanostructured carbons [13,45–48] so that the whole MnO_2 material participates.

5. Conclusion

In this study, manganese dioxide crystallized in the γ-MnO_2 phase was prepared by hydrothermal method. The electrodeposition of PPy on prepared MnO_2 was carried out with chronoamperometry test at different times. The BET surface area of PPy/MnO_2 is larger than that measured with prepared MnO_2 by 51.2%. The presence of PPy improves the electrochemical performance of the composite material electrode and increases the specific capacitance. The electrochemical studies reveal that the electrode performance of the composite material (PPy/MnO_2) as an electrode material prepared after 40 min, defined as the specific capacitance per gram of the composite, reaches 141.6 F g^{-1}, against 73.7 F g^{-1} before coating. These results well compare with results obtained on α-MnO_2 with the same porosity. In addition, while the coating with PPy is known to improve the capacitance due to the beneficial effect of its electronic conductivity, we find that the main effect is actually due to the fact that PPy increases the pore accessibility in the mesoporous MnO_2 electrode. The porosity is thus the crucial parameter that determines the intrinsic electrochemical of this material.

References

[1] A. Rudge, J. Davey, I. Raistrick, S. Gottesfeld, J.P. Ferraris, J. Power Sources 47 (1994) 89.
[2] A. Rudge, I. Raistrick, S. Gottesfeld, J.P. Ferraris, Electrochim. Acta 39 (1994) 273.
[3] B.E. Conway, in: Electrochemical Supercapacitors: Scientific Fundamentals and Technological Applications, Springer, 1999.
[4] M. Mastragostino, F. Soavi, R. Arbizzani, Electrocapacitors in Advances in Lithium-ion Batteries, Springer, 2002.
[5] H.S. Kim, N. Branko, B.N. Popov, J. Power Sources 104 (2002) 52.
[6] H.Y. Lee, J.B. Goodenough, J. Solid State Chem. 144 (1999) 220.
[7] M. Toupin, T. Brousse, D. Bélanger, Chem. Mater. 16 (2004) 3184.
[8] V. Subramanian, H. Zhu, B. Wei, J. Power Sources 159 (2006) 361.
[9] A. Izadi-Najafabadi, S. Yasuda, K. Kobashi, K.T. Yamada, D.N. Futaba, H. Hatori, M. Yumura, S. Iijima, K. Hata, Adv. Mater. 22 (2010) E235.
[10] Z.-S. Wu, W. Ren, D.-W. Wang, F. Li, B. Liu, H.-M. Cheng, ACS Nano 4 (2010) 5835.
[11] S. Chen, J. Zhu, X. Wu, Q. Han, X. Wang, ACS Nano 4 (2010) 2822.
[12] S. Devaraj, N. Munichandraiah, Electrochem. Solid-State Lett. 8 (2005) A373.
[13] E. Raymundo-Pinero, V. Khomenko, E. Frackowiak, F. Beguin, J. Electrochem. Soc. 152 (2005) A229.
[14] D. Bélanger, T. Brousse, J.W. Long, Interface 17 (2008) 49.
[15] R.N. Reddy, R.G. Reddy, J. Power Sources 132 (2004) 315.
[16] H. Kim, B.N. Popov, J. Electrochem. Soc. 150 (2003) D56.
[17] D. Bélanger, T. Brousse, J.W. Long, Electrochem. Soc. Interfaces 17 (2008) 49.
[18] K. Naoi, P. Simon, Electrochem. Soc. Interfaces 17 (2008) 34.
[19] X. Lang, A. Hirata, T. Fujita, M. Chen, Nat. Nanotechnol. 6 (2011) 232.
[20] S.-B. Ma, K.-W. Nam, W.-S. Yoon, X.-Q. Yang, K.-Y. Ahn, K.-H. Oh, K.-B. Kim, J. Power Sources 178 (2008) 483.
[21] S.R. Sivakkumar, J.M. Ko, D.Y. Kim, B.C. Kim, G.G. Wallace, Electrochim. Acta 52 (2007) 7377–7385.
[22] S.W. Lee, J. Kim, S. Chen, P.T. Hammond, Y. Shao-Horn, ACS Nano 4 (2010) 3889.
[23] L. Hu, M. Pasta, F.L. Mantia, L. Cui, S. Jeong, H.D. Deshazer, J.W. Choi, S.M. Han, Y. Cui, Nano Lett. 10 (2010) 708.
[24] J. Yan, Z. Fan, T. Wei, W. Qian, M. Zhang, F. Wei, Carbon 48 (2010) 3825.
[25] G. Yu, L. Hu, M. Vosgueritchian, H. Wang, X. Xie, J.R. McDonough, X. Cui, Y. Cui, Z. Bao, Nano Lett. 11 (2011) 2905.
[26] R. Liu, S.B. Lee, J. Am. Chem. Soc. 130 (2008) 2942.
[27] L. Chen, L.-J. Sun, F. Luan, Y. Liang, Y. Li, X.-X. Liu, J. Power Sources 195 (2010) 3742.
[28] T. Brousse, M. Toupin, R. Dugas, L. Athouel, O. Crosnier, D. Bélanger, J. Electrochem. Soc. 153 (2006) A2171.

[29] G.H. Du, Z.Y. Yuan, G. Van Tendeloo, Appl. Phys. Lett. 86 (2005) 063113.
[30] X. Wang, Y. Li, Chem. Commun. (2002) 764.
[31] C. Ye, Z.M. Lin, S.Z. Hui, J. Electrochem. Soc. 152 (2005) A1272.
[32] H. Groult, C.M. Julien, A. Bahloul, S. Leclerc, E. Briot, A. Mauger, Electrochem. Commun. 13 (2011) 1074.
[33] J.O. Besenhard, Handbook of Battery Materials, Wiley-VCH GmbH, 1999.
[34] A. Bahloul, B. Nessark, F. Habelhames, C.M. Julien, Ionics 17 (2011) 239.
[35] T.A. Skotheim, R.L. Elsenbaumer, J.R. Reynolds, Handbook of Conducting Polymers Second Edition, Marcel Dekker Inc., 1998.
[36] A. Bahloul, B. Nessark, N.E. Chelali, H. Groult, A. Mauger, C.M. Julien, Solid State Ionics 204–205 (2011) 53.
[37] H.Y. Lee, S.W. Kim, H.Y. Lee, Electrochem. Solid-State Lett. 4 (2001) A19.
[38] J.N. Broughton, M.J. Brett, Electrochim. Acta 50 (2005) 4814.
[39] J.K. Chang, C.T. Lin, W.T. Tsai, Electrochem. Commun. 6 (2004) 666.
[40] G.X. Wang, B.L. Zhang, Z.L. Yu, M.Z. Qu, Solid State Ionics 176 (2005) 1169.
[41] Y. Hou, Y. Cheng, T. Hobson, J. Liu, Nano Lett. 10 (2010) 2727–2733.
[42] T. Brezesinski, J. Wang, S.H. Tolbert, B. Dunn, Nat. Mater. 9 (2010) 146.
[43] S.-C. Pang, M.A. Anderson, T.W. Chapman, J. Electrochem. Soc. 147 (2000) 444.
[44] J.N. Broughton, M.J. Brett, Electrochim. Acta 49 (2004) 4439.
[45] V. Subramanian, H. Zhu, B. Wei, Electrochem. Commun. 8 (2004) 827.
[46] C.Y. Lee, H.M. Tsai, H.J. Chuang, S.Y. Li, P. Lin, Y.T. Tseng, J. Electrochem. Soc. 152 (2005) A716.
[47] Y.-T. Wu, C.-C. Hu, J. Electrochem. Soc. 151 (2004) A2060.
[48] X. Dong, W. Shen, J. Gu, L. Xiong, Y. Zhu, H. Li, J. Shi, J. Phys. Chem. B 110 (2006) 6015.